Effect of Substitution Position of Dibenzofuran-terminated Robust Hole- transporters on Physical Properties and TADF OLED Performances

Journal:	*Molecular Systems Design & Engineering*
Manuscript ID	ME-ART-10-2022-000225.R2
Article Type:	Paper
Date Submitted by the Author:	22-Nov-2022

Complete List of Authors:	Abe, Shoki; Yamagata Daigaku, Organic Device Engineering Sasabe, Hisahiro; Yamagata Daigaku, Organic Device Engineering Nakamura, Takeru; Yamagata Daigaku, Organic Device Engineering Matsuya, Misaki; Yamagata Daigaku, Organic Device Engineering Saito, Yu; Yamagata Daigaku, Organic Device Engineering Hanayama, Takanori; Yamagata Daigaku, Organic Device Engineering Araki, Suguru; Yamagata Daigaku, Organic Device Engineering Kumada, Kengo; Yamagata Daigaku, Organic Device Engineering Kido, Junji; Yamagata Daigaku, Organic Device Engineering

‘Design, System, Application’ statement

Although the wide-energy-gap hole-transport layer (HTL) is a key material to realizing high-efficiency and long-lifetime phosphorescent and thermally activated delayed fluorescent (TADF) organic light-emitting devices (OLEDs), a limited number of HTLs have been explored in previous studies. Among HTLs, dibenzofuran-end-capped HTLs show promising performances in highly efficient and stable OLEDs. This study investigates the effects of the substitution positions of **TnDBFBP** (n=1–4) derivatives with four DBF-end-capping groups to extensively study the molecular design of robust multifunctional HTLs. **TnDBFBP** derivatives exhibited a high glass transition temperature (T_g) of ~149℃, triplet energy (ET) value of ~2.9 eV, and anionic bond dissociation energy of ~1.75 eV depending on the substitution positions. Consequently, **T1DBFBP** realized green TADF OLEDs with an EQE of over 20% and an operational lifetime (LT_{50}) of 30000 h at 1000 cd/m^2. These performances are among the best reported by previous studies. We believe that this study provides fundamental guidelines to develop thermally and electrically stable hole-transporters as well as high-efficiency OLEDs with long term stability.

Effect of Substitution Position of Dibenzofuran-terminated Robust Hole-transporters on Physical Properties and TADF OLED Performances

Shoki Abe,[1] *Hisahiro Sasabe,**[1,2,3] *Takeru Nakamura,*[1] *Misaki Matsuya,*[1] *Yu Saito,*[1] *Takanori Hanayama,*[1] *Suguru Araki,*[1] *Kengo Kumada,*[1] *and Junji Kido**[1,2,3]

[1]Department of Organic Materials Science, Yamagata University, 4-3-16 Jonan, Yonezawa, Yamagata 992-8510, Japan, [2]Research Center of Organic Electronics (ROEL), Yamagata University, 4-3-16 Jonan, Yonezawa, Yamagata 992-8510, Japan, and [3]Frontier Center for Organic Materials (FROM), Yamagata University, 4-3-16 Jonan, Yonezawa, Yamagata 992-8510, Japan

Academic titles: Prof. Hisahiro Sasabe, Mr. Shoki Abe, Mr. Takeru Nakamura, Ms. Misaki Matsuya, Mr. Yu Saito, Mr. Takanori Hanayama, Mr. Suguru Araki, Mr. Kengo Kumda, Prof. Junji Kido

*Corresponding author
E-mail: h-sasabe@yz.yamagata-u.ac.jp

Keywords: organic light-emitting devices; thermally activated delayed fluorescence; long lifetime; hole-transporter; arylamine derivative

Abstract: Although the wide-energy-gap hole-transport layer (HTL) is a key material to realizing high-efficiency and long-lifetime phosphorescent and thermally activated delayed fluorescent (TADF) organic light-emitting devices (OLEDs), a limited number of HTLs have been explored in previous studies. Accordingly, dibenzofuran-end-capped HTLs show promising performance in realizing a maximum external quantum efficiency (EQE) of 20% and a long lifetime of over 20000 h at 1000 cd/cm^2 in phosphorescent and TADF OLEDs. This study investigates the effects of the substitution positions of **TnDBFBP** (n=1–4) derivatives with four DBF-end-capping groups to extensively study the molecular design of robust multifunctional HTLs. **TnDBFBP** derivatives exhibited a high glass transition temperature (T_g) of ~149˚C, triplet energy (E_T) value of ~2.9 eV, and anionic bond dissociation energy of ~1.75 eV depending on the substitution positions. Consequently, **T1DBFBP** realized green TADF OLEDs with an EQE of over 20% and an operational lifetime of 50% of the initial luminance (LT_{50}) of 30000 h at 1000 cd/m^2. These performances are among the best reported by previous studies.

Introduction

High-performance organic light-emitting devices (OLEDs) are among the most vital technologies for small-to-large-area displays and illumination light sources [1,2]. OLEDs are multilayer structures consisting of a hole-transport layer (HTL), an emissive layer (EML), and an electron-transport layer (ETL) to realize high efficiency and long lifetime. Among the three primary layers, the weak electrochemical stability of the HTL toward the anion state is known to be a major bottleneck in lifetime prolongation[3], particulary for thermally activated delayed fluorescent (TADF) and phosphorescent OLEDs, where high triplet energy (E_T) materials are imperative to confine all the molecular excitons of singlets and triplets. In addition, the high morphological stability of thin films at temperatures above 100 °C is necessary for practical applications [3c]. The most famous HTL, **NPD**, has a low glass transition temperature (T_g) of 96 °C and an E_T value of 2.3 eV [4], which is not applicable for green and blue TADF and phosphorescent OLEDs. Thus, a thermally and electrochemically robust high-E_T HTL is necessary to realize high-efficiency, long-lifetime OLEDs. However, the number of reported robust high-E_T HTLs is limited. For example, Nakanotani et al. reported a carbazole trimer named **TrisPCz** with a T_g of 154˚C and E_T of 2.65 eV[5]. **TrisPCz** realized efficient and long-lifetime green TADF and phosphorescent OLEDs. Fukagawa et al. developed a dibenzofuran-end-capped HTL, named **4DBFP3Q**, with *a* T_g of 103 °C and E_T of 2.59 eV[6]. **4DBFP3Q** realized green phosphorescent OLEDs with an external quantum efficiency (EQE) of 21% and an operational lifetime of 50% of the initial luminance (LT_{50}) of over 10000 h at 1000 cd/m^2.

In our previous studies, we observed that the introduction of DBF-end-capping groups significantly increased the anionic bond dissociation energy (BDE) of the C-N bond, and four DBF-end-capping HTLs, such as **T4DBFBP** and **T4DBFHPB**, successfully realized high-efficiency and long-lifetime TADF and phosphorescent OLEDs with an EQE of over 20% and LT_{50} of over 20000 h at a high brightness of 1000 cd/m^2[7] (**Table S1**). To extensively study the molecular design of robust high-E_T HTLs, we investigated the effect of the substitution

positions of **TnDBFBP** derivatives with four DBF-end-capping groups. **TnDBFBP** derivatives exhibited a high T_g of ~149˚C, E_T of ~2.9 eV, and anionic BDE of ~1.75 eV depending on the substitution position. Notably, the ionization potential can be tuned from 5.5 to 5.9 eV. Consequently, among the **TnDBFBP** derivatives, **T1DBFBP** realized green TADF OLEDs with an EQE of over 20% and LT_{50} of 30000 h at 1000 cd/m^2. These performances are among the best reported in previous studies.

Results and discussion

Molecular design, quantum chemical calculations, and preparation of TnDBFBP

Although the performances of DBF-end-capping HTLs in realizing high-efficiency and long-lifetime TADF and phosphorescent OLEDs are promising, only 4-position derivatives have been used from the viewpoints of high E_T, large anionic BDE, deep ionization potential (I_P), and synthetic availability[7,8]. As shown in **Figure 1**, DBF has four positions for possible chemical modifications. Bis(dibenzofuran-n-yl)aniline monomers (n=1–4) (**M1–4)** were displayed using Corey-Pauling-Koltun (CPK) models in **Figure 1** to understand the structural characteristics of the triarylamine moiety in the target molecules. **M1** and **M4** had a more twisted structure with a lower conjugation length, induced by the bent structure of DBF, compared with that of **M2** and **M3**. The nitrogen atom at the center of triarylamine was covered by DBF moieties. In contrast, DBF moieties in **M2** and **M3** were connected in a relatively linear manner, resulting in a longer conjugation length.

Subsequently, we designed and investigated the effect of the substitution positions of **TnDBFBP** derivatives (n=1–4), corresponding to the dimer of **M1-4**, on OLED performance. Note that the properties of **T4DBFBP** (n=4) have been partially reported in the separated paper.[7] We selected the biphenyl skeleton and *meta*-conjugation to increase the E_T values to confine the triplet excitons of the green TADF emitter and prevent crystallization induced by

the π-π stacking of large DBF moieties. The molecular weight (MW) of all derivatives was 849 g/mol.

First, we conducted density functional theory (DFT) calculations using Gaussian09[9] (**Figure 2**) to estimate the optoelectronic properties, such as the highest occupied molecular orbital (HOMO)/lowest unoccupied molecular orbital (LUMO), energy gap, and triplet energy (E_T). The HOMO levels considerably changed depending on the substitution positions, and the order of the values was **2** ≈ **3** > **4** > **1**. The HOMOs were distributed on the triphenyl amine moieties, whereas the LUMOs were distributed on DBF moieties. The order of E_T values was **1** > **4** > **2** > **3**, depending on the conjugation length. Here, these four derivatives are approximately divided into two groups: (a) **1** and **4** and (b) **2** and **3**. Highly twisted molecular structures were obtained for HTLs **1** and **4** because of the bent structures of the DBF moieties. Conversely, less twisted molecular structures were obtained for HTL **2** and **3**. In addition, the conjugation lengths increased owing to the *para*-position of the oxygen atom toward the nitrogen atom for **2**, and the *para*-biphenyl moiety toward the nitrogen atom for **3**. As previously pointed out, the BDE of HTL in the anion state is one of the bottleneck to shorten the stability of **4CzIPN**-based devices because the carriers are accumulated at the HTL/EML interface.[8] Therefore, the BDEs in the anion states were then calculated as a fundamental physical property according to a previously reported method[10]. All derivatives resulted in relatively large BDE values > 1.43 eV compared with triphenyl amine (BDE_{anion} = 0.87 eV, **Table S2**). HTL **2** exhibited the largest BDE value of 1.75 eV, most likely resulting from the longer conjugation length. Conversely, the BDE value of HTL **1** was the smallest (1.43 eV), presumably because of steric repulsions from the highly twisted molecular structure (**Figure S1**). In addition, the BDE values in the neutral state, which is homolytic dissociation, were calculated to be similar values of around 3.2 eV (**Figure S2**).

Target materials **1–4** were prepared using the Buchwald-Hartwig amination reaction (**Scheme S1**). First, the corresponding primary amine was coupled with brominated DBF to obtain a

secondary amine of 46–82% yield. Subsequently, the obtained secondary amine was coupled with m-dibromobiphenyl to obtain **TnDBFBP** derivatives of 29–85% yield. These derivatives were further purified using the train sublimation technique and fully characterized using ^{1}H- and ^{13}C-NMR, mass spectrometry, and elemental analyses (**Figure S3–14**). The purity of the materials was confirmed to be >99.5% using ultra-performance liquid chromatography before device fabrication.

Thermal and photophysical properties

Thermal properties were measured using thermogravimetric analysis (TGA) and differential scanning calorimetry (DSC) (**Figure S15–20**). Temperatures of 5% weight loss (T_{d5}) were observed above 450 °C, and glass transition temperatures (T_g) were observed above 135 °C, indicating the high thermal stability of these derivatives in the solid-state film. Among **TnDBFBP** derivatives, less twisted molecular structures such as **2** and **3 resulted in** higher T_g values, probably because of stronger intermolecular packing, whereas the twisted structure with weaker intermolecular packing, such as **4**, resulted in a lower T_g value. Therefore, **1**, with a twisted structure, exhibited a significantly different tendency to show the highest T_g value. This suggests that the oxygen atoms on the outer sphere of the molecule play an essential role in strengthening the intermolecular interaction using multiple CH-O weak hydrogen bonds[11]. All **TnDBFBP** derivatives were sublimable under a vacuum.

Ultraviolet–visible absorption and photoluminescence spectra were measured for the thin solid film state (**Figure S21**). As predicted in the DFT calculations, HTL **1** and **4** showed much shorter absorption edge and peak emission wavelengths compared with those of HTL **2** and **3** because of the shorter conjugation length. The low-temperature photoluminescence spectra at 5 K were also measured (**Figure S22**). All derivatives exhibited relatively high E_T >2.6 eV, which was estimated from the onset of phosphorescence. The ionization potentials (I_P) were measured by photoelectron yield spectrometry. Based on the DFT calculations, the I_P values

changed significantly depending on the substitution position and ranged between 5.5 and 5.9 eV. Twisted structures with shorter conjugation lengths, such as **1** and **4**, had deep I_P values, whereas less twisted structures with longer conjugation lengths, such as **2** and **3**, had shallow I_P values. Hole mobilities were measured using the time-of-flight technique. The results of hole mobilities of the **TnDBFPB** derivatives are shown in **Figure 3** and **S23**. Hole mobilities significantly changed and ranged from 10^{-5} to 10^{-3} cm^2/Vs, depending on the substitution positions. HTL **2** and **3** with longer conjugation lengths exhibited higher mobility compared with that of hexaphenylbenzene-based **4DBFHPB** (1.5×10^{-3} cm^2/Vs)[8b], whereas HTL **1** and **4** showed 1/10 lower mobility. Further, the order of the reorganization energies of cation state (λ) were calculated to be **T3** (68 meV) < **T4** (110 meV) ~ **T2** (113 meV) < **T1** (121 meV) (**Table S3**). The λ values of **T1**, **T2**, and **T4** were almost similar, and there was no strong relationship between hole mobilities and λ values except **T3**. Although the molecular orientation is one of the key parameters to change the mobility, however, we were not able to determine the order parameters (*S*) due to the flexible molecular structure with a large number of conformers derived from *meta*-conjugation.[7] The thermal and photophysical properties are summarized in **Table 1**.

OLED performances

To evaluate the performance of **TnDBFBP** derivatives, we fabricated **4CzIPN**-based green TADF OLEDs with the following structure: [ITO (100 nm)/ polymer buffer[12] (20 nm)/ **NPD** (10 nm)/ **HTL** (10 nm)/ 3,3'-Di(9H-carbazol-9-yl)-1,1'-biphenyl (**mCBP**)[13]: 20wt% **4CzIPN** (30 nm)/ 2-(3'-(dibenzo[b,d]thiophen-4-yl)-[1,10-biphenyl]-3-yl)-4,6-diphenyl-1,3,5-triazine (**DBF-TRZ**)[14] (10 nm)/ 2,9-bis(naphthalen-2-yl)-4,7-diphenyl-1,10-phenanthroline (**nBPhen**) (40 nm)/8-quinolinolato lithium (**Liq**) (2 nm)/Al (100 nm)]. Here, we used **nBPhen** as an ETL because this ETL is expected to realize longer lifetime[15] compared with previously

used **DPB**.[7] The chemical structures and energy diagrams are shown in **Figure 4**. The device performances are summarized in **Table 2**. The EL spectra of the devices, clearly showing the emission only from **4CzIPN** are shown in **Figure 5a**. The current density-luminance-voltage (*J–V–L*) characteristics are shown in **Figure 5b**. HTLs with an intermediate I_P value of 5.75 eV between **mCBP** (6.0 eV) and **NPD** (5.5 eV) exhibited a greater current density and luminance. Therefore, stepwise hole injection, while maintaining a larger overlap of the density-of-states [16] of both **mCBP** and **NPD** is key to decreasing the driving voltages. The external quantum efficiency-luminance (*EQE-L*) characteristics are shown in **Figure 5c**. HTL **1**, with both deep I_P and high E_T values, recorded the highest EQEs of up to 21%, whereas HTLs with shallower I_P and E_T values exhibited lower EQEs. In particular, HTLs with a shallower I_P of 5.6 eV resulted in EQEs below 10% at a low luminance of 1 cd/m^2. HTLs with a shallow I_p can form exciplexes with **4CzIPN**, resulting in quenching at the HTL/EML interface[5]. To further investigate the quenching at HTL/EML interface, photoluminescent quantum yield (PLQY) of double layer films with the structure of quartz/HTL (10 nm)/ **mCBP**: 20wt% **4CzIPN** (100 nm) were investigated. When the excitation light with the wavelength of 350 nm was used, the **4CzIPN**/**mCBP** films inserted with **TnDBFBP** exhibited PLQY values of 62–87%. PLQY values were decreased in the order of **T4** (87%) > **T1** (84%) > **T2** (81%) > **T3** (62%), which was almost correlated with the I_p values. The lifetimes were measured at a constant current density of 10 mA/cm^2, which corresponded to a luminance of approximately 5300–6200 cd/m^2 (**Figure 5d**). We then carried out the acceleration test at the constant current density of 20 and 30 mA/cm^2 (**Figure S24**). The operation lifetime at the initial luminance (L_0) of 1000 cd/m^2 was estimated by these luminance acceleration tests based on the formula $L_0^n \times LT(L_0) = const.$[17]. These values are the highest among **4CzIPN**-based OLEDs [5,7,8,18]. The lifetimes increased when HTLs with deeper I_P were used; particularly, HTL **1**, with a deep I_P of 5.9 eV and high E_T of 2.8 eV, showed the best lifetime among **TnDBFBP** derivatives. Therefore, the reduced charge accumulation between the HTL and EML by controlling the alignment of I_p

values decreased the exciplex formation and chemical degradation of HTL, thus enhancing EQEs and lifetimes.

Conclusion

Among the wide-gap HTLs in previous studies, DBF-end-capped HTLs exhibit promising performance in realizing high-efficiency and long-lifetime TADF and phosphorescent OLEDs. Consequently, to extensively study the relationship between the chemical structure, optoelectronic properties, and device performance, we prepared four types of structural isomers, **TnDBFBP** (n=1–4), and investigated the effect of the substitution positions of DBF-end-capping groups. All derivatives were easily prepared on a gram scale via two-step palladium-catalyzed Buchwald-Hartwig reactions. The **TnDBFBP** derivatives exhibited completely different optoelectronic properties of I_P, E_T, BDE, and mobility, depending on the substitution positions. HTL **1** and **4** had twisted structures induced by the bent structure of DBF units and less conjugation lengths compared with those of HTL **2** and **3**. Thus, HTL **1** and **4** showed deeper I_P values ~5.9 eV, higher E_T >2.7 eV, and lower mobility ~10^{-5} cm^2/Vs. However, HTL **2** and **3** showed shallower I_P values ~5.5 eV, lower E_T ~2.6 eV, and higher mobility up to 2.6 x 10^{-3} cm^2/Vs. Notably, I_P values can be tuned from 5.5 to 5.9 eV depending on the substitution position. For thermal properties, these derivatives exhibited a high T_g of over 135 °C, indicating high morphological stability in the solid film. Finally, among the **TnDBFPB** derivatives, HTL **1** with deep I_P values of 5.9 eV and high E_T of 2.8 eV could reduce the charge accumulation at the HTL/EML interface and realize green TADF OLEDs with an EQE of over 20% and LT_{50} of 30000 h at a high brightness of 1000 cd/m^2. These performances are among the best reported in previous studies. The results reveal the significance of the HTL/EML interface in increasing the efficiency and lifetime of OLEDs.

Supporting Information

Supporting information is available.

Acknowledgments

We gratefully acknowledge the partial financial support from the Center of Innovation (COI) Program of the Japan Science and Technology Agency (JST) and the subsidy program for the development of advanced research infrastructure from the Ministry of Education, Culture, Sports, Science, and Technology (MEXT). In addition, H.S. acknowledges the partial financial support from JSPS KAKENHI (20H02807) from the Japan Society for the Promotion of Science (JSPS).

References

[1] (a) C. Adachi, *Jpn. J. Appl. Phys.* **2014**, *53*, 060101; (b) Z. Yang, Z. Mao, Z. Xie, Y. Zhang, S. Liu, J. Zhao, J. Xu, Z. Chi, M. P. Aldred, *Chem. Soc. Rev.* **2017**, *46*, 915; (c) Y. Im, M. Kim, Y. J. Cho, J.-A Seo, K. S. Yook, J. Y. Lee, *Chem. Mater.* **2017**, *29*, 1946; (d) M. Y. Wong, E. Z.-Colman, *Adv. Mater.* **2017**, *29*, 1605444; (e) R. Komatsu, H. Sasabe, J. Kido, *J. Phon. Ener.* **2018**, *8*, 032108; (f) H. Kaji, H. Suzuki, T. Fukushima, K. Shizu, K. Suzuki, S. Kubo, T. Komino, H. Oiwa, F. Suzuki, A. Wakamiya, Y. Murata, C. Adachi, *Nat. Commun.* **2015**, *6*, 8476; (g) T. Hatakeyama, K. Shiren, K. Nakajima, S. Nomura, S. Nakatsuka, K. Kinoshita, J. Ni, Y. Ono, T. Ikuta, *Adv. Mater.* **2016**, *28*, 2777.

[2] (a) W. Song and J. Y. Lee, *Adv. Opt. Mater.*, **2017**, *5*, 1600901; (b) K. H. Kim and J. J. Kim, *Adv. Mater.*, **2018**, *30*, 1705600; (c) S. Scholz, D. Kondakov, B. Lüssem, and K. Leo, *Chem. Rev.,* **2015**, *115*, 8449; (d) G. Li, Z. Q. Zhu, Q. Chen, J. Li, *Org. Electron.*, **2019**, *69*, 135; (e) Y. Wang, J. H. Yun, L. Wang, and J. Y. Lee, *Adv. Funct. Mater.*, **2021**, *31*, 2008332; (f) T. Chatterjee and K.T. Wong, *Adv. Optical Mater.*, **2019**, 7, 1800565; (g) Y. Watanabe, H. Sasabe, J. Kido, *Bull. Chem. Soc. Jpn.* **2019**, *92*, 716.

[3] (a) D. Y. Kondakov, *J. Appl. Phys*. **2008**, *104*, 084520; (b) S. Schmidbauer, A. Hohenleutner, B. König, *Adv. Mater*. **2013**, *25*, 2114; (c) S. S. Swayamprabha, D. K. Dubey, Shanawaz, R. A. K. Yadav, M. R. Nagar, A. Sharma, F.-C. Tung, J.-H. Jou, *Adv. Sci.* **2021**, *8*, 2002254.

[4] H. Fukagawa, T. Shimizu, Y. Kiribayashi, Y. Osada, T. Kamada, T. Yamamoto, N. Shimidzu, T. Kurita, *Appl. Phys. Lett.* **2013**, *103*, 143306.

[5] H. Nakanotani, K. Masui, J. Nishide, T. Shibata, C. Adachi, *Sci. Rep.* **2013**, *3*, 2127.

[6] H. Fukagawa, T. Shimizu, H. Kawano, S. Yui, T. Shinnai, A. Iwai, K. Tsuchiya, T. Yamamoto, *J. Phys. Chem. C* **2016**, *120*, 18748.

[7] (a) H. Sasabe, S. Araki, S. Abe, N. Ito, K. Kumada, T. Noda, Y. Sukegawa, D. Yokoyama, J. Kido, *Chem. Eur. J.* **2022**, *13*, e202104408; (b) N. Nagamura, H. Sasabe, H. Sato, T.

Kamata, N. Ito, S. Araki, S. Abe, Y. Sukegawa, D. Yokoyama, H. Kaji, J. Kido, *J. Mater. Chem. C* **2022**, *10*, 8694.

[8] (a) T. Kamata, H. Sasabe, M. Igarashi, J. Kido, *Chem. Eur. J.* **2018**, *24*, 4590; (b) T. Kamata, H. Sasabe, N. Ito, Y. Sukegawa, A. Arai, T. Chiba, D. Yokoyama, J. Kido, *J. Mater. Chem. C* **2020**, *8*, 7200.

[9] *Gaussian 09*, Revision D.01, M. J. Frisch, G. W. Trucks, H. B. Schlegel, G. E. Scuseria, M. A. Robb, J. R. Cheeseman, G. Scalmani, V. Barone, B. Mennucci, G. A. Petersson, H. Nakatsuji, M. Caricato, X. Li, H. P. Hratchian, A. F. Izmaylov, J. Bloino, G. Zheng, J. L. Sonnenberg, M. Hada, M. Ehara, K. Toyota, R. Fukuda, J. Hasegawa, M. Ishida, T. Nakajima, Y. Honda, O. Kitao, H. Nakai, T. Vreven, J. A. Montgomery, Jr., J. E. Peralta, F. Ogliaro, M. Bearpark, J. J. Heyd, E. Brothers, K. N. Kudin, V. N. Staroverov, R. Kobayashi, J. Normand, K. Raghavachari, A. Rendell, J. C. Burant, S. S. Iyengar, J. Tomasi, M. Cossi, N. Rega, J. M. Millam, M. Klene, J. E. Knox, J. B. Cross, V. Bakken, C. Adamo, J. Jaramillo, R. Gomperts, R. E. Stratmann, O. Yazyev, A. J. Austin, R. Cammi, C. Pomelli, J. W. Ochterski, R. L. Martin, K. Morokuma, V. G. Zakrzewski, G. A. Voth, P. Salvador, J. J. Dannenberg, S. Dapprich, A. D. Daniels, Ö. Farkas, J. B. Foresman, J. V. Ortiz, J. Cioslowski, and D. J. Fox, Gaussian, Inc., Wallingford CT, 2013.

[10] (a) N. Lin, J. Qiao, L. Duan, L. Wang, Y. Qiu, *J. Phys. Chem. C.* **2014**, *118*, 7569; (b) M. Hong, M. K. Ravva, R. Winget, J.-L. Brédas, *Chem. Mater.* **2016**, *28*, 5791.

[11] G. R. Desiraju, T. Steiner, The Weak Hydrogen Bond–In Structural Chemistry and Biology. Oxford University Press (1999).

[12] J. Kido, G. Harada, M. Komada, H. Shionoya, K. Nagai, *ACS. Synp. Ser.* **1997**, *672*, 381.

[13] P. Schrögel, N. Langer, C. Shildknecht, G. Wagenblast, C. Lennartz, P. Strohriegl, *Org. Electron.* **2011**, *12*, 2047.

[14] (a) Y. Nagai, H. Sasabe, J. Takahashi, N. Onuma, T. Ito, S. Ohisa, J. Kido, *J. Mater. Chem. C* **2017**, *5*, 527; (b) T. Ito, H. Sasabe, Y. Nagai, Y. Watanabe, N. Onuma, J. Kido, *Chem. Eur. J.* **2019**, *25*, 7308.

[15] H. Tsuneyama, H. Sasabe, Y. Saito, T. Noda, D. Saito, J. Kido, *J. Mater. Chem. C* **2022**, *10*, 2073.

[16] T. Matsushima, K. Goushi, C. Adachi, *Chem. Phys. Lett.* **2007**, *435*, 327.

[17] C. Féry, B. Racine, D. Vaufrey, H. Doyeux, S. Cinà, *App. Phys. Lett.* **2005**, *87*, 213502.

[18] L. S. Cui, S. B. Ruan, F. Bencheikh, R. Nagata, L. Zhang, K. Inada, H. Nakanotani, L. S. Liao, C. Adachi, *Nat Commun* **2017**, *8*, 2250.

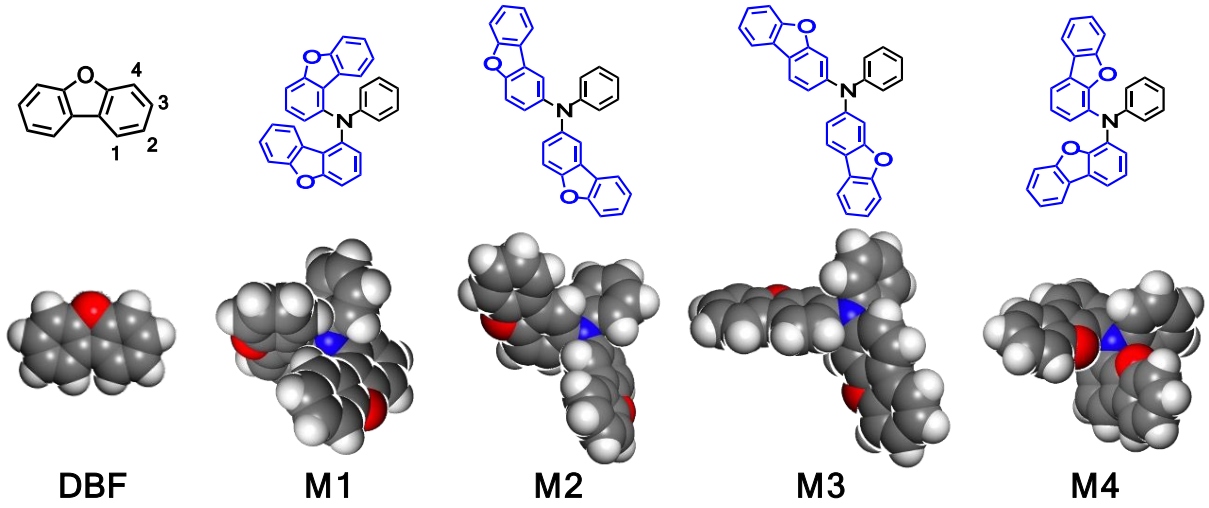

Figure 1. The substitution position of dibenzofuran (DBF) and the chemical structures of bis(dibenzofuran-n-yl)aniline monomer (n=1–4) displayed using the CPK model.

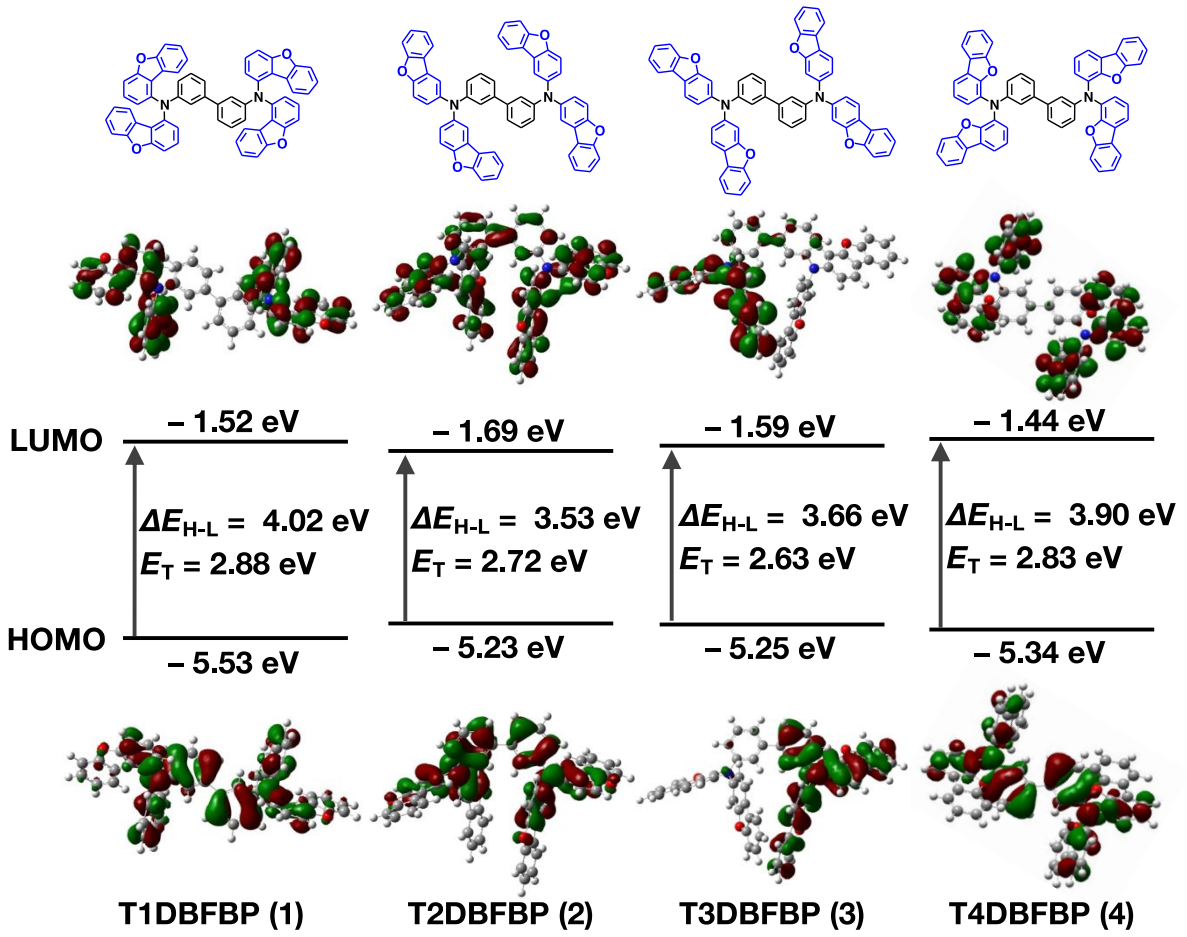

Figure 2. HOMO and LUMO distributions and energy levels; HOMO-LUMO energy differences (ΔE_{H-L}); lowest triplet energy (E_T) for **TnDBFBP** derivatives.

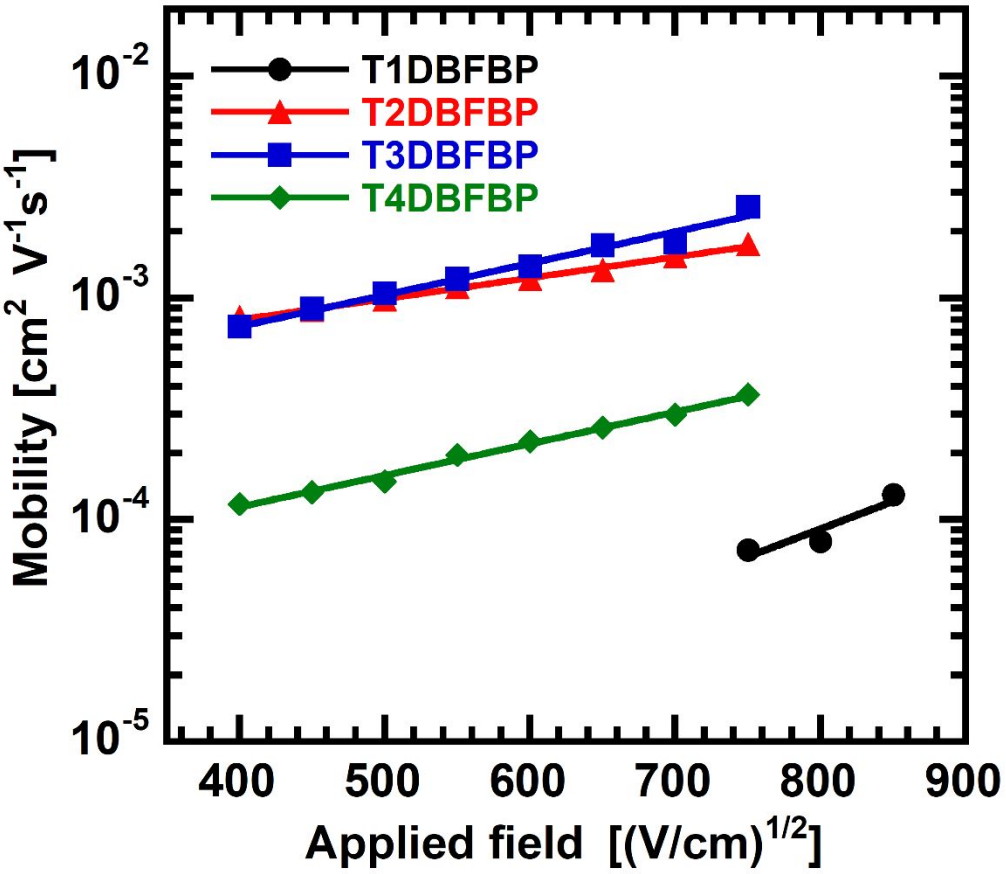

Figure 3. Hole mobilities plotted with respect to $E^{1/2}$ for **TnDBFPB** derivatives.

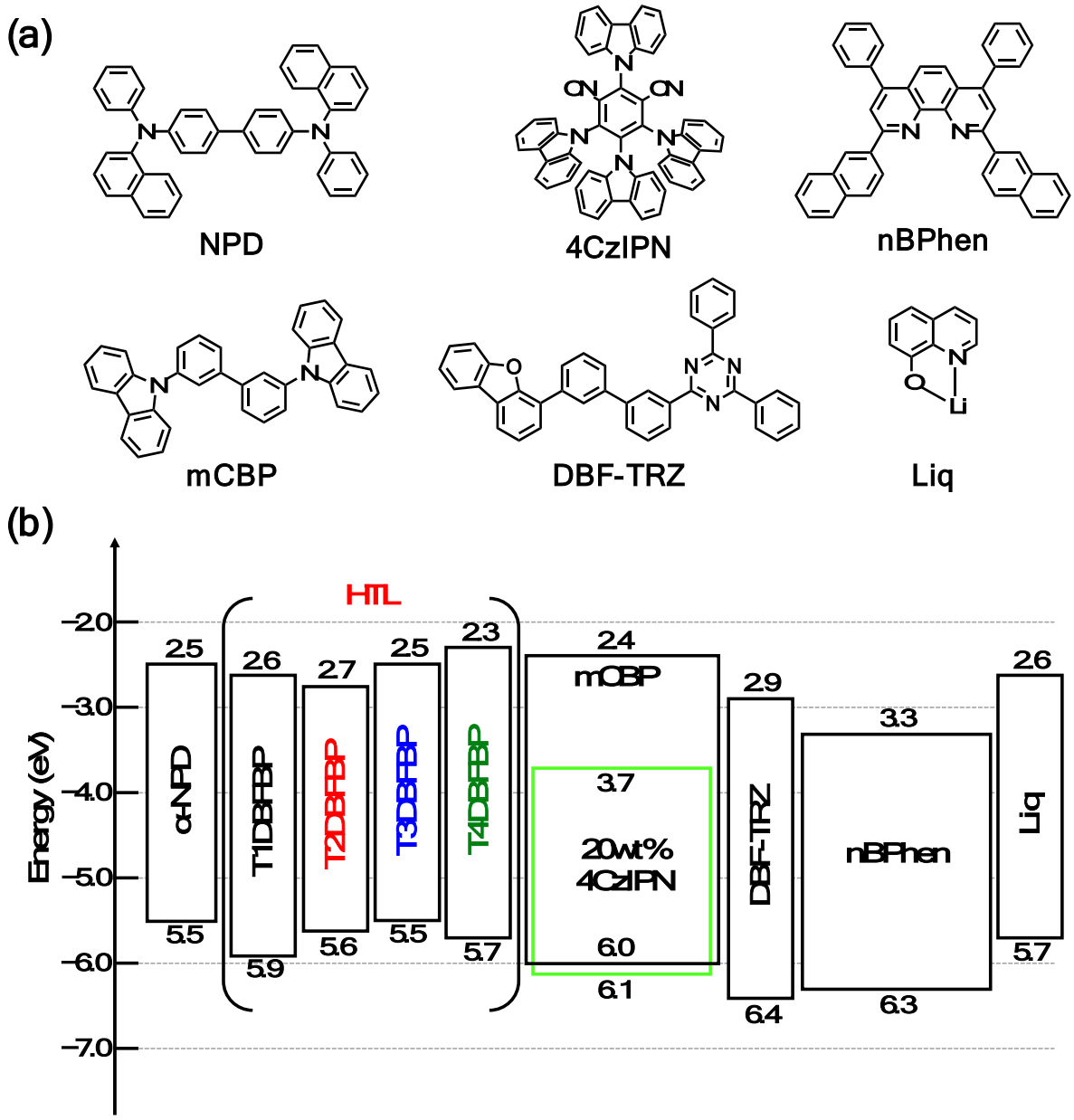

Figure 4. (a) Chemical structures of materials used in OLEDs. (b) Energy diagram of OLEDs.

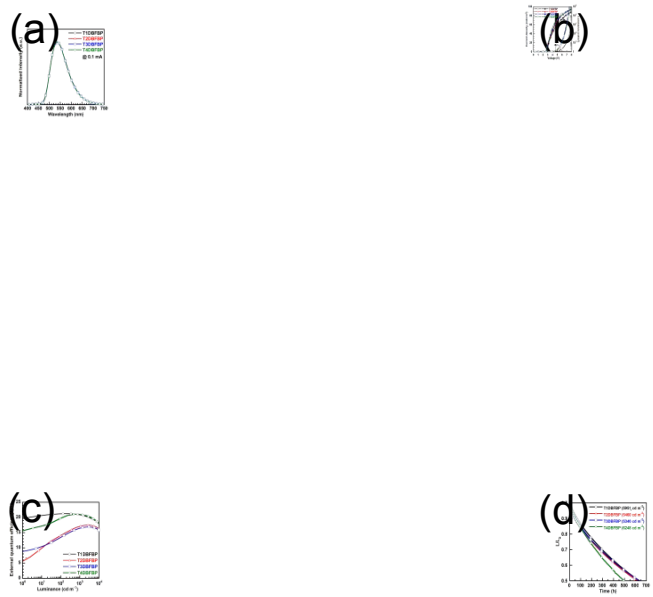

Figure 5. Device performance of green TADF OLEDs: a) EL spectra; b) *J-V-L* characteristics; c) *EQE-L* characteristics; d) operation lifetime at 10 mA cm^{-2}.

Table 1. Thermal and optical properties.

Compound	MW	T_g[a]/T_m[a]/T_{d5}[b] (ºC)	HOMO[c]/LUMO[c]/E_T[d] (eV)	I_p[e]/E_g[f]/E_a[g]/E_T[h] (eV)
T1DBFBP	849	149/290/465	−5.53/−1.52/2.88	5.9/3.2/2.6/2.8
T2DBFBP	849	144/303/511	−5.23/−1.69/2.72	5.6/2.9/2.7/2.7
T3DBFBP	849	145/330/532	−5.25/−1.59/2.63	5.5/3.0/2.5/2.6
T4DBFBP	849	138/286/493	−5.34/−1.44/2.83	5.7/3.4/2.3/2.7

[a]T_g and T_m were determined using DSC. [b]T_{d5} was determined using TGA. [c,d]Calculated at the B3LYP/ 6-311+G(d,p)// B3LYP 6-31G(d) level. [d]Calculated triplet energy. [e]I_p was determined using photoelectron yield spectroscopy. [f]E_g was considered the point at which the normalized absorption spectra intersected. [g]E_a was calculated using I_p and E_g. [h]E_T was estimated from the onset of the phosphorescent spectra at 5 K.

Table 2. Summary of OLED performances.

HTM	V_{on}[a] (V)	V_{1000}/ $\eta_{c,1000}$/ $\eta_{p,1000}$/ $\eta_{ext,1000}$[b] (V/cd A^{-1}/lm W^1/%)	LT_{50} at 10 mA cm^{-2} (h)[c]	LT_{50} at 1000 cd m^{-2} (h)[d]
T1DBFBP	2.82	4.94/70.9/45.1/20.9	636	~30,000
T2DBFBP	2.63	4.55/58.0/40.0/17.1	626	~24,000
T3DBFBP	2.69	4.46/55.8/39.3/16.4	639	~25,000
T4DBFBP	2.60	4.26/71.5/52.8/21.0	497	~27,000

[a]Turn-on voltage at 1 cd m^{-2}, [b]current efficiency (η_c), power efficiency (η_p), and EQE (η_{ext}) at 1000 cd m^{-2}. [c]Operation lifetime at 50% (LT_{50}) at a constant current density of 10 mA cm^{-2}. [d]LT_{50} of 1000 cd m^{-2}, estimated using the luminance acceleration test.